Supplementary Information

Introducing Phenol-yne Chemistry for the Design of Lignin-based Vitrimers: Towards Sustainable and Recyclable Materials

Lisa Sougrati [a], Antoine Duval [a, b,*], Luc Avérous [a,*]

[a] BioTeam/ICPEES-ECPM, UMR CNRS 7515, Université de Strasbourg, 25 rue Becquerel, 67087 Strasbourg Cedex 2, France

[b] Soprema, 15 rue de Saint Nazaire, 67100 Strasbourg, France

* Prof. Luc Avérous, Phone: + 33 368852784, Fax: + 33 368852716, E-mail: luc.averous@unistra.fr

* Dr Antoine Duval, E-mail: antoine.duval@unistra.fr

Characterization of lignins

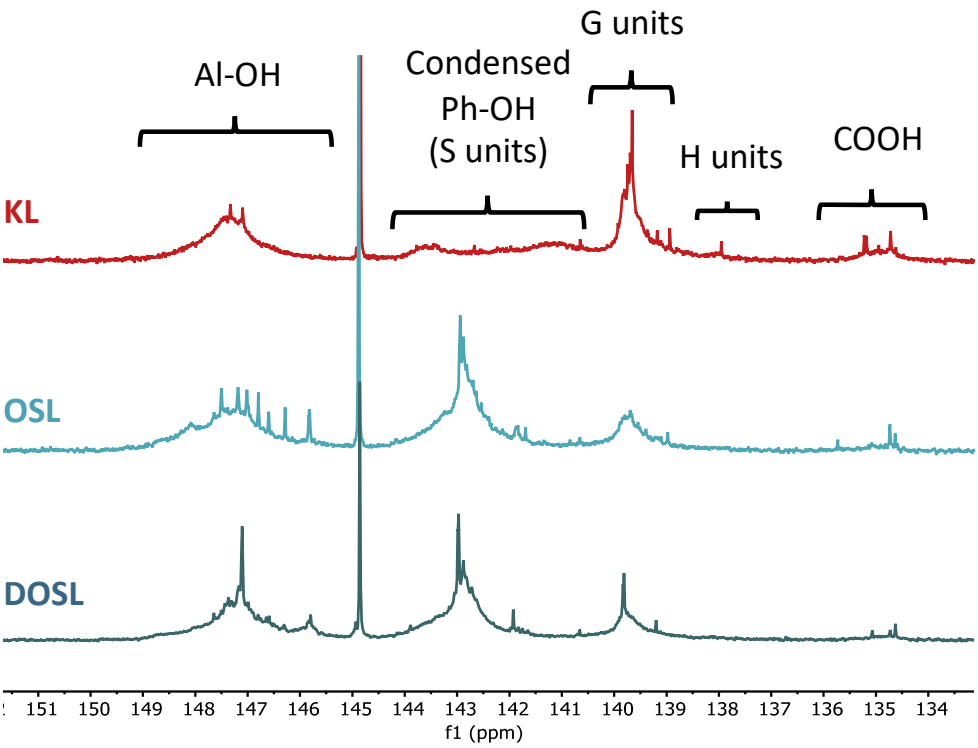

Figure S1. ^{31}P NMR spectra of KL, OSL, and DOSL.

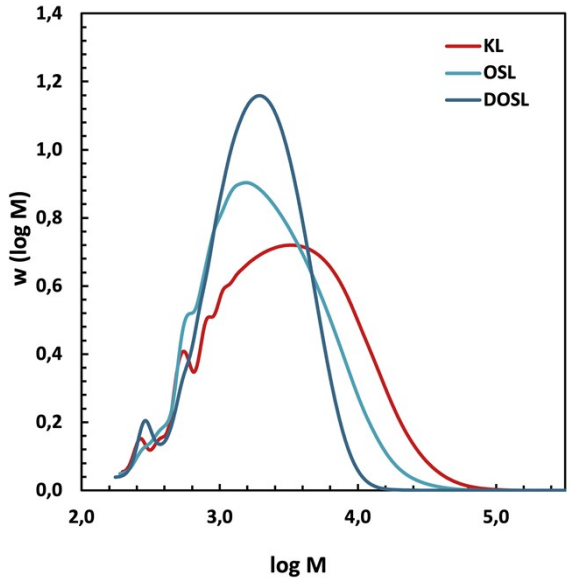

Figure S2. SEC distributions of KL, OSL, and DOSL (acetylated lignins, THF as eluent, PS standards).

Synthesis of small molecule models

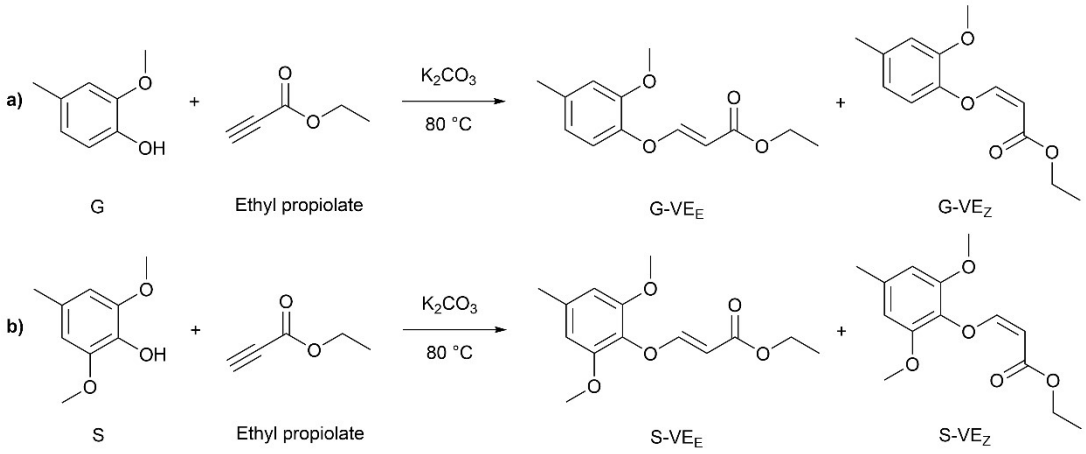

Scheme S 1. Synthesis of G-VE and S-VE model compounds by click-addition.

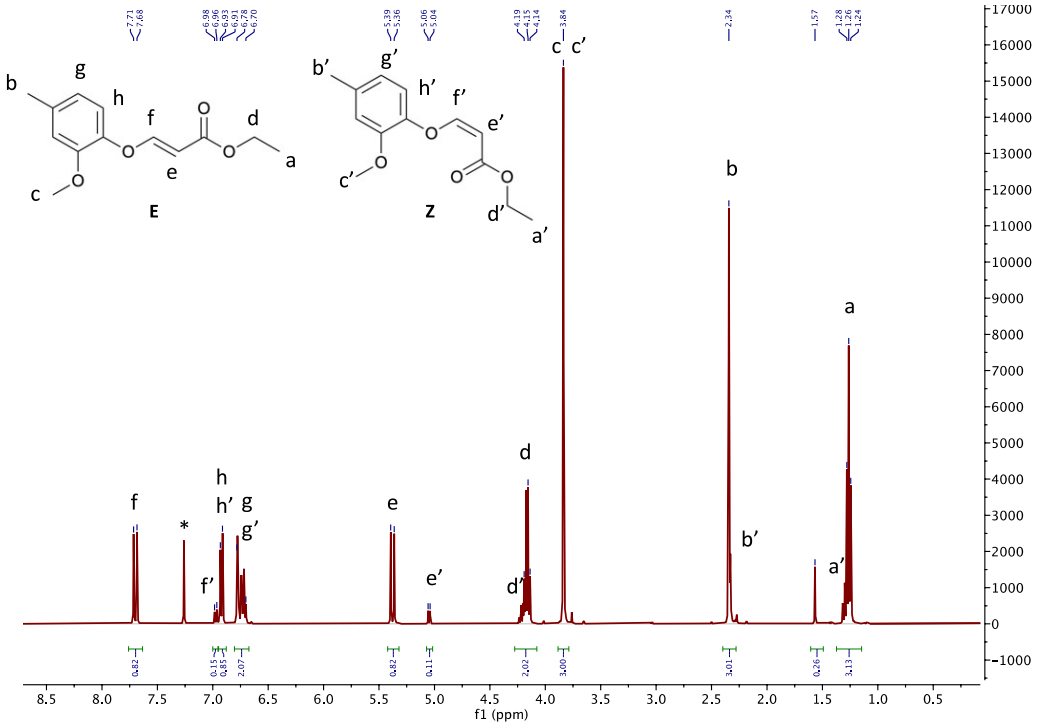

Figure S3. ^{1}H NMR of G-VE in $CDCl_3$.

^{1}H NMR (400 MHz, $CDCl_3$) δ 7.70 (d, J = 12.2 Hz, 1H), 6.92 (d, J = 7.9 Hz, 1H), 6.78 (s, 2H), 5.38 (d, J = 12.3 Hz, 1H), 4.28 – 4.08 (m, 2H), 3.84 (s, 3H), 2.34 (s, 3H), 1.26 (t, J = 7.2 Hz, 3H).

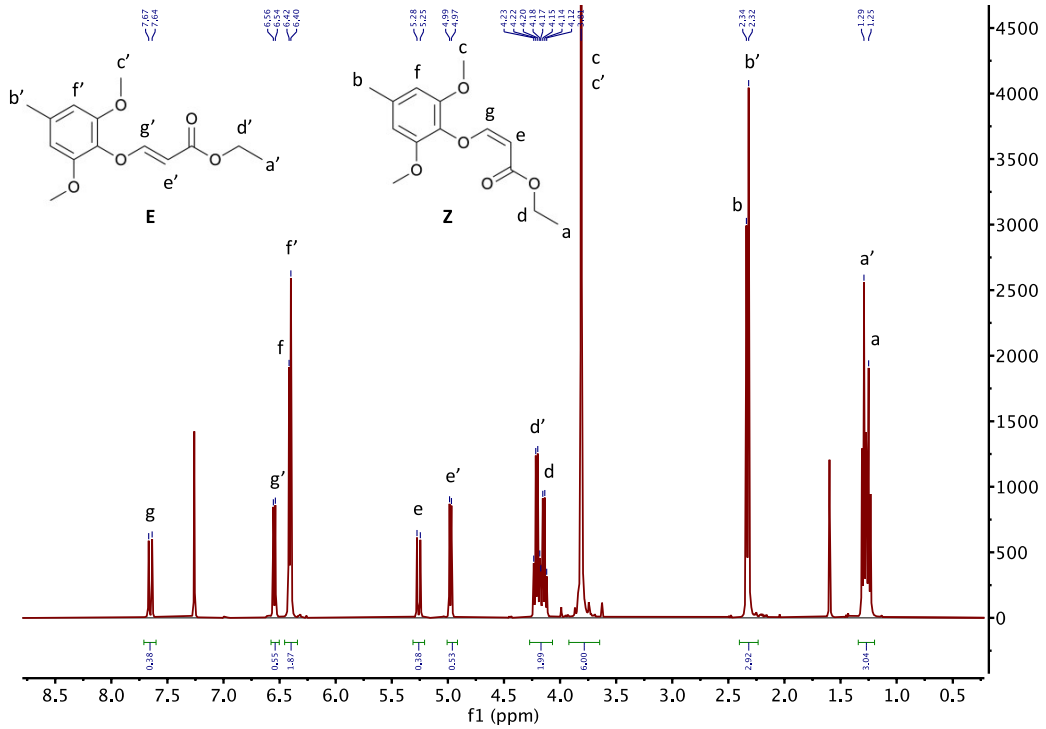

Figure S4. ^{1}H NMR of S-VE in $CDCl_3$.

^{1}H NMR (400 MHz, $CDCl_3$) δ 7.65 (d, *J* = 12.2 Hz, 1H), 6.55 (d, *J* = 7.0 Hz, 1H), 5.26 (d, *J* = 12.2 Hz, 1H), 4.98 (d, *J* = 7.0 Hz, 1H), 4.21 (q, *J* = 7.2 Hz, 3H), 4.15 (q, *J* = 7.2 Hz, 2H), 1.27 (d, *J* = 16.5 Hz, 4H).

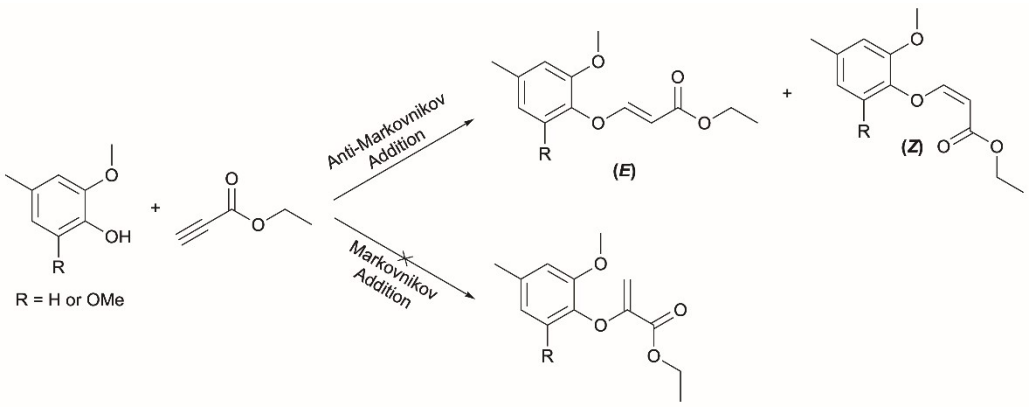

Scheme S2. Markovnikov and anti-Markovnikov additions of ethyl propiolate and phenols. Only the anti-Markovnikov product is obtained.

Study of exchange reactions on small molecule models

Table S1. Vinyl ether model exchange reactions conditions.

Exchange units	Model	Exchangeable unit	m_{model} (g)	Quantity exch. unit	m_{K2CO3} (g)
GG'	G-VE	G'	0.2	93 µL	0.0059
GS'	G-VE	S'	0.2	0.1304 g	0.0059
SG'	S-VE	G'	0.2	83 µL	0.0052
SS'	S-VE	S'	0.2	0.1158 g	0.0052
G/Al	G-VE	Benzyl alcohol	0.2	88 µL	0.0059
Al/G	Benz	G	1	613 µL	0.0335

System GG'

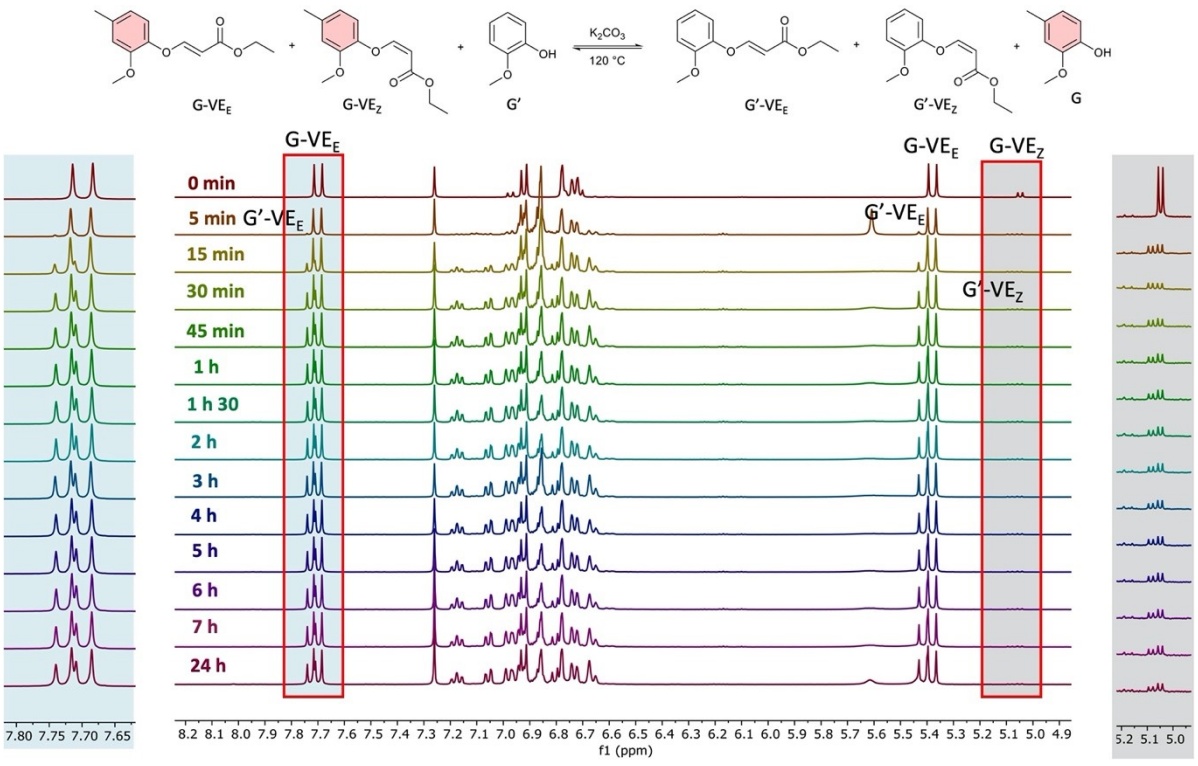

Figure S5. ^{1}H NMR sequence of GG' exchange reaction between G-VE and G in $CDCl_3$.

$$K_{GG'} = \frac{[G'\text{-}VE][G]}{[G\text{-}VE][G']} = 0.29$$

Table S2. Parameters used for $K_{GG'}$ calculation.

Compound	ppm	Area	Relative area	Molar fraction
G-VE[a]	5.04-5.06 (*Z*) 7.68-7.71 (*E*)	34409	34409	0.34
G'	3.89	95568	31855	0.31
G'-VE[a]	5.08-5.09 (*Z*) 7.71-7.74 (*E*)	18077	18077	0.18
G	3.87	52621	17540	0.17

[a]Sum of *E* and *Z*-isomers.

System SS'

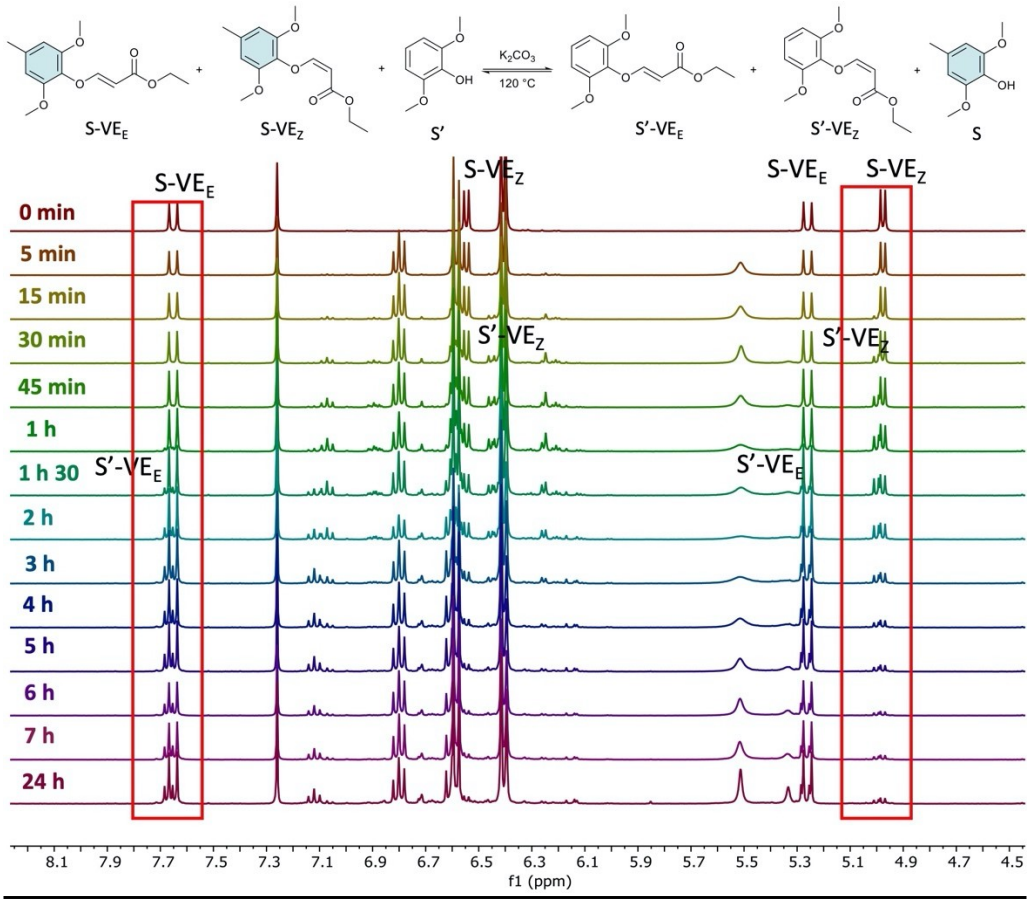

Figure S6. ^{1}H NMR sequence of SS' exchange reaction between S-VE and S' in $CDCl_3$.

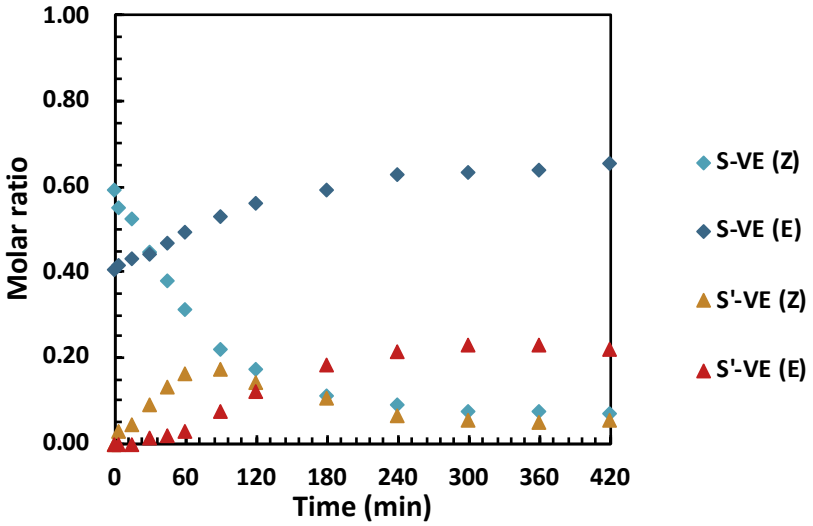

Figure S7. Kinetics of SS' exchange reaction between S-VE and S' at 120 °C.

$$K_{SS'} = \frac{[S'\text{-}VE][S]}{[S\text{-}VE][S']} = 0.18$$

Table S3. Parameters used for $K_{SS'}$ calculation.

Compound	ppm	Area	Relative area	Molar fraction
S-VE[a]	4.97-4.99 (*Z*) 7.64-7.67 (*E*)	39383	39383	0.31
S'	3.89	292905	48817	0.39
S'-VE[a]	4.99-5.01 (*Z*) 7.65-7.68 (*E*)	15351	15351	0.12
S	3.87	134776	22463	0.18

[a]Sum of *E* and *Z*-isomers.

System GS'

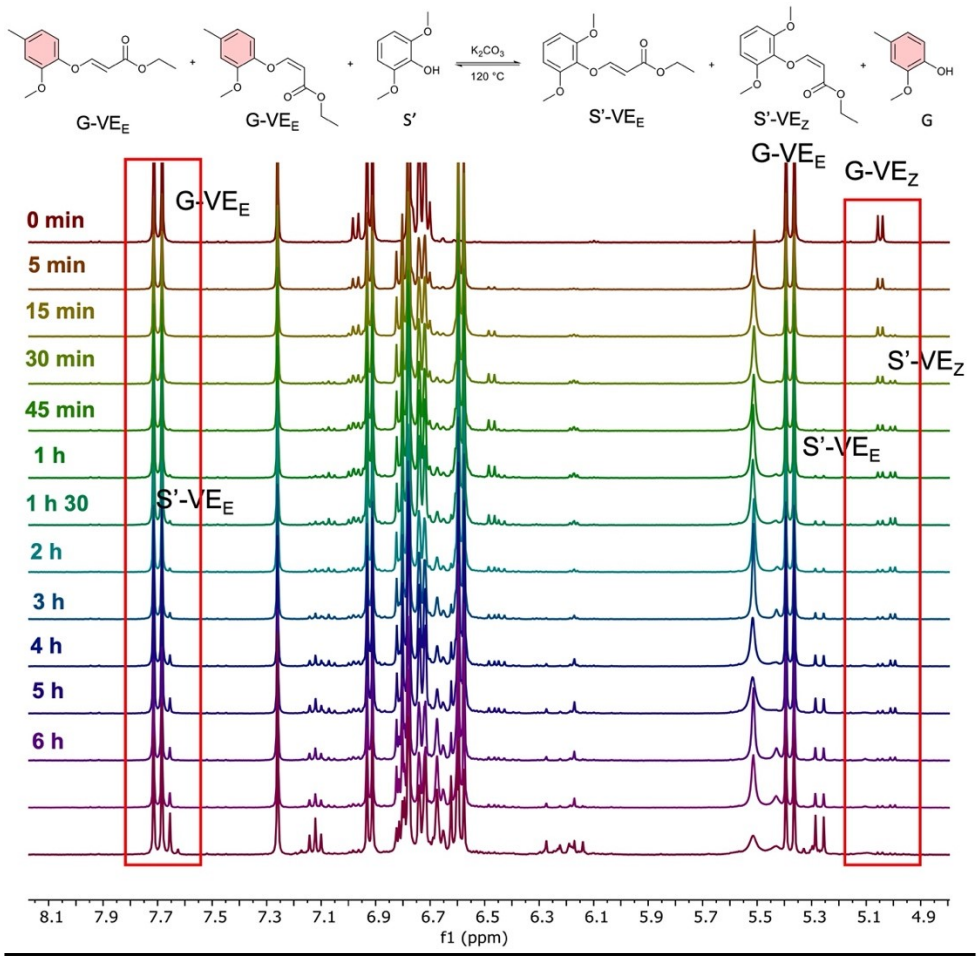

Figure S8. ^{1}H NMR sequence of GS' exchange reaction between G-VE and S' in $CDCl_3$.

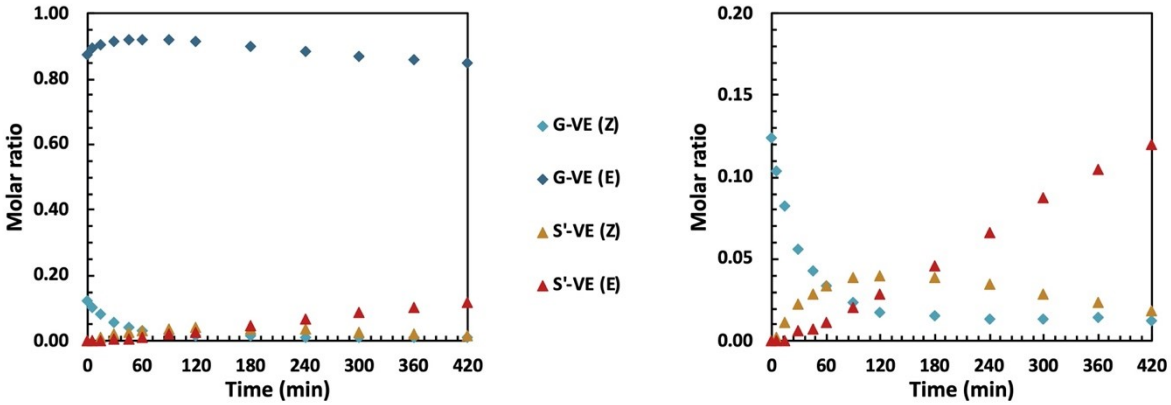

Figure S9. Kinetics of GS' exchange reaction between G-VE and S' at 120 °C, with zoom on molar ratios from 0 to 0.2.

$$K_{GS'} = \frac{[S'\text{-}VE][G]}{[G\text{-}VE][S']} = 0.27$$

Table S4. Parameters used for $K_{GS'}$ calculation.

Compound	ppm	Area	Relative area	Molar fraction
G-VE[a]	5.04-5.06 (*Z*) 5.36-5.39 (*E*)	44277	44277	0.45
S’	3.89	133929	22321	0.22
S’-VE[a]	4.99- 5.01 (*Z*) 5.26-5.29 (*E*)	14888	14888	0.15
G	3.87	54015	18005	0.18

[a]Sum of *E* and *Z*-isomers.

System SG'

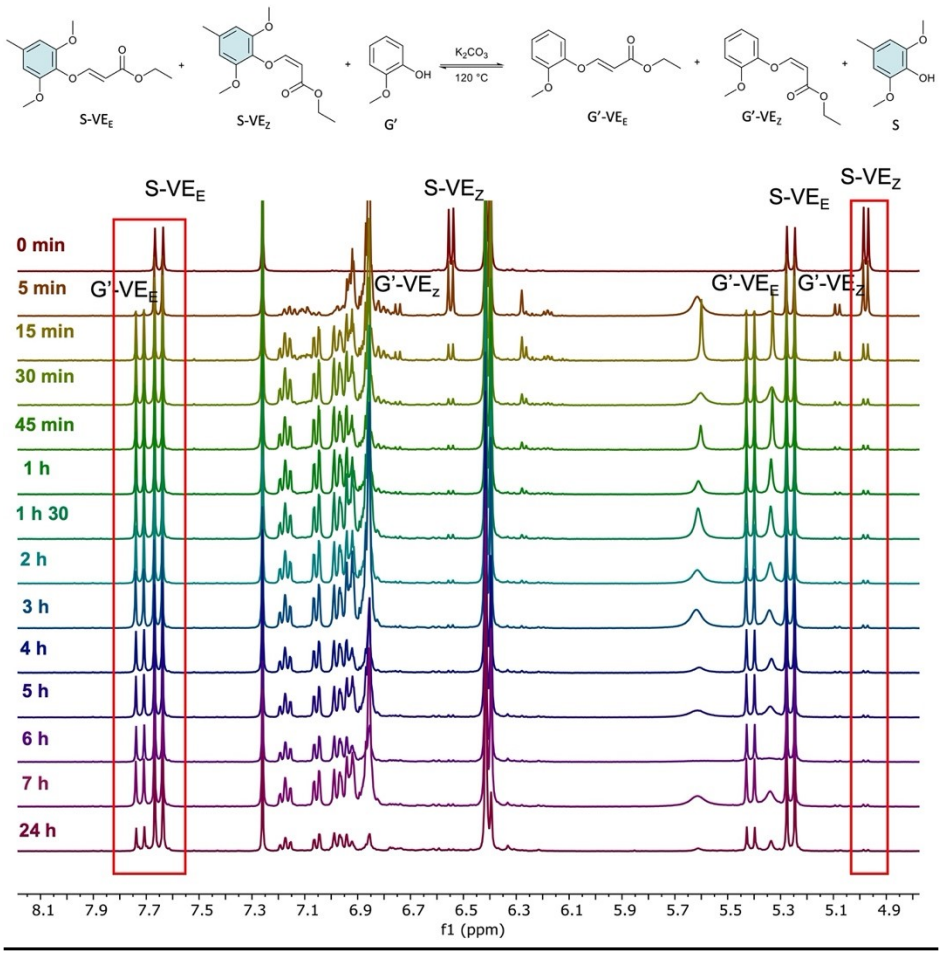

Figure S10. ^{1}H NMR sequence of SG' exchange reaction between S-VE and G' in $CDCl_3$.

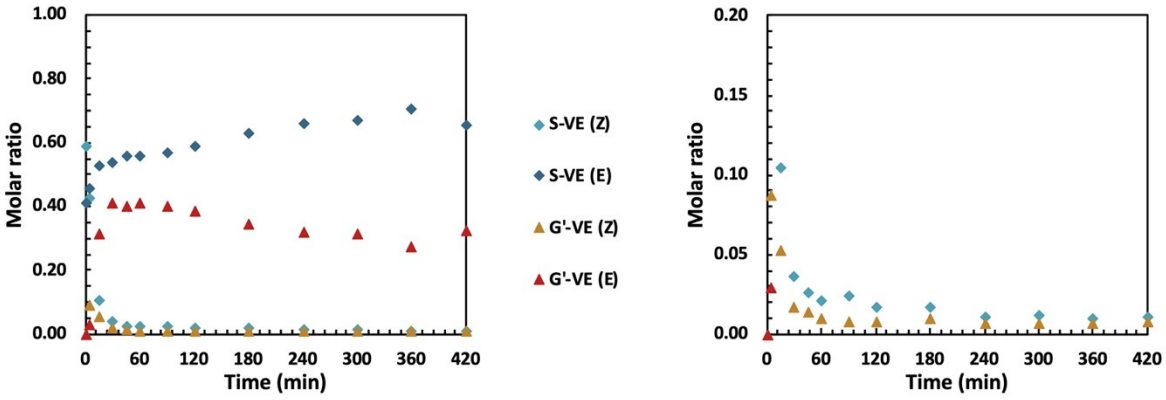

Figure S11. Kinetics of SG' exchange reaction between S-VE and G' at 120 °C, with zoom on molar ratios from 0 to 0.2.

$$K_{SG'} = \frac{[G'\text{-}VE][S]}{[S\text{-}VE][G']} = 0.37$$

Table S5. Parameters used for $K_{SG'}$ calculation.

Compound	ppm	Area	Relative area	Molar fraction
S-VE[a]	4.97-4.99 (*Z*) 7.64-7.67 (*E*)	38245	38245	0.34
G’	3.89	95568	31856	0.28
G’-VE[a]	5.08-5.09 (*Z*) 7.71-7.74 (*E*)	19049	19049	0.17
S	3.87	141778	23626	0.21

[a]Sum of *E* and *Z*-isomers.

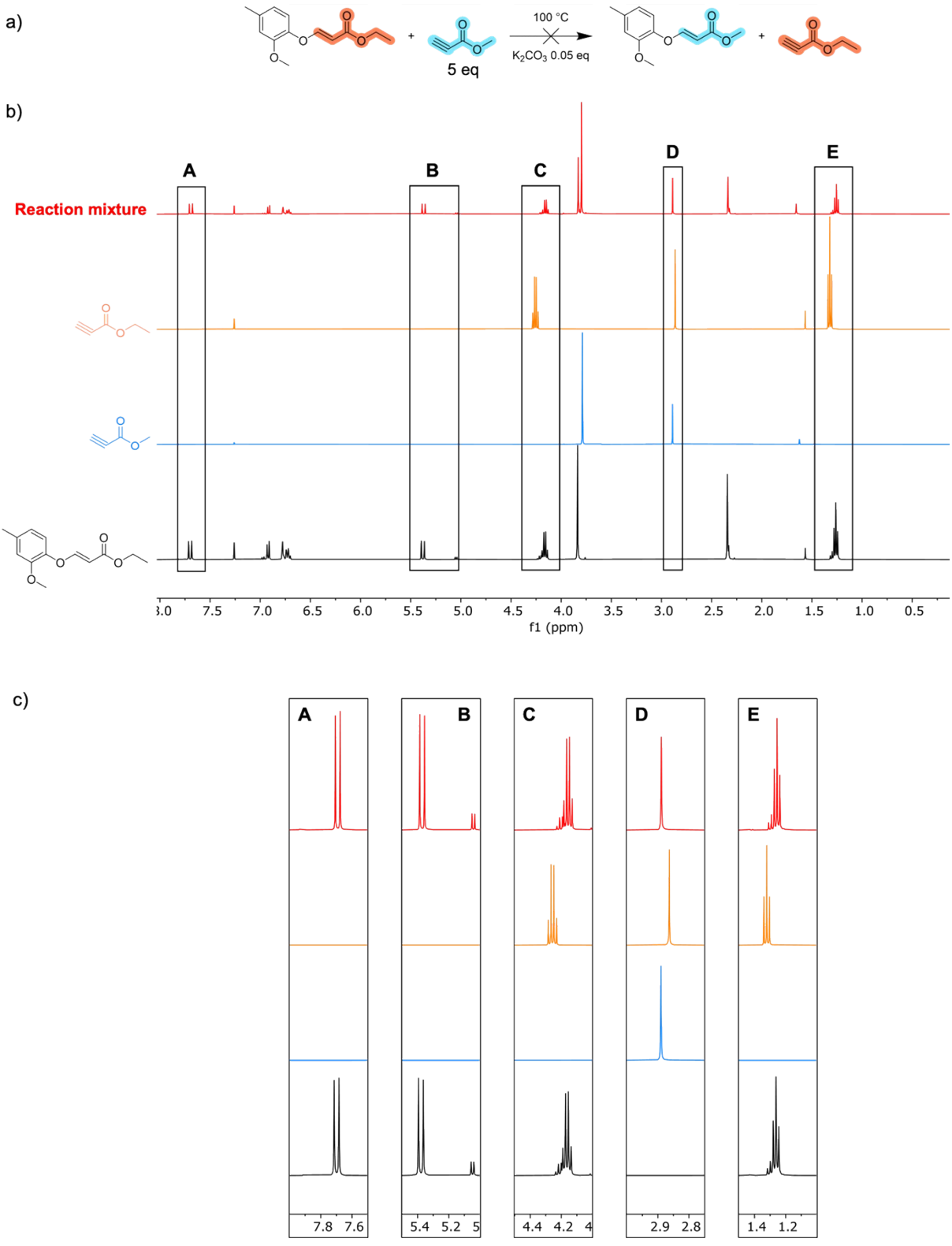

Figure S 12. Reaction performed to test dissociative exchange mechanism: a) scheme of the reaction between model G-VE and excess methyl propiolate, b) ^{1}H NMR spectra of the reaction mixture, showing only G-VE and methyl propiolate, and the absence of exchange products (spectrum of ethyl propiolate is provided for comparison), c) details of relevant regions of the ^{1}H NMR spectra.

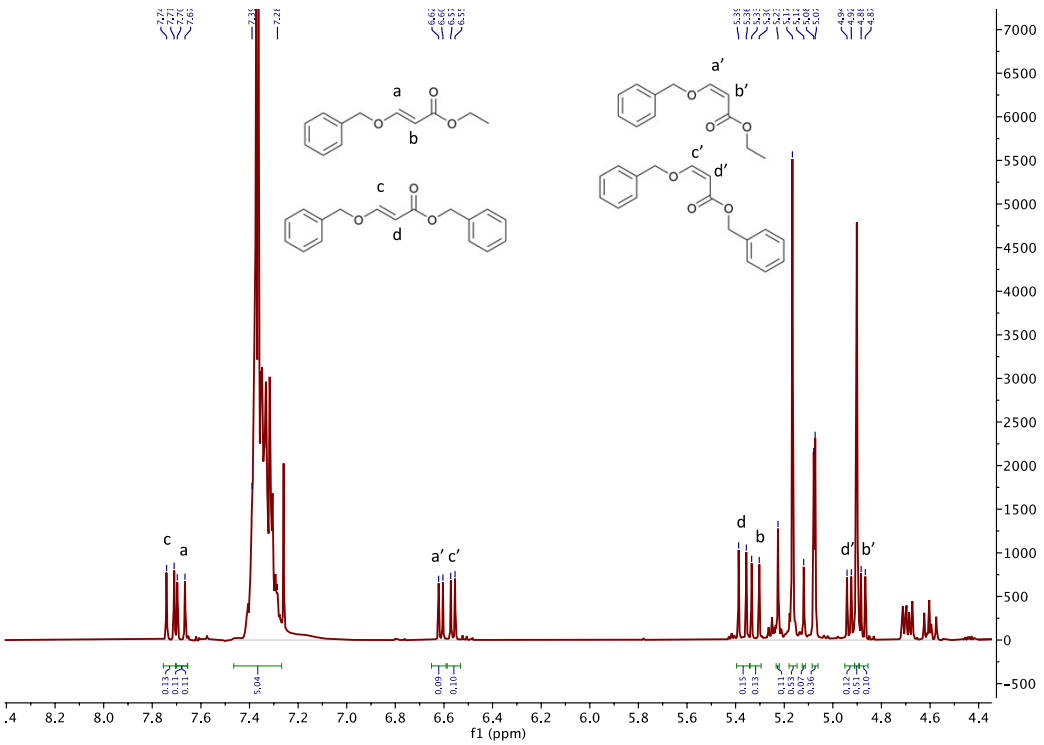

Figure S13. ^{1}H NMR of the reaction of benzyl alcohol with ethyl propiolate at 120 °C in $CDCl_3$ and proposition for the attribution of possible product from click-addition and transesterification reactions.

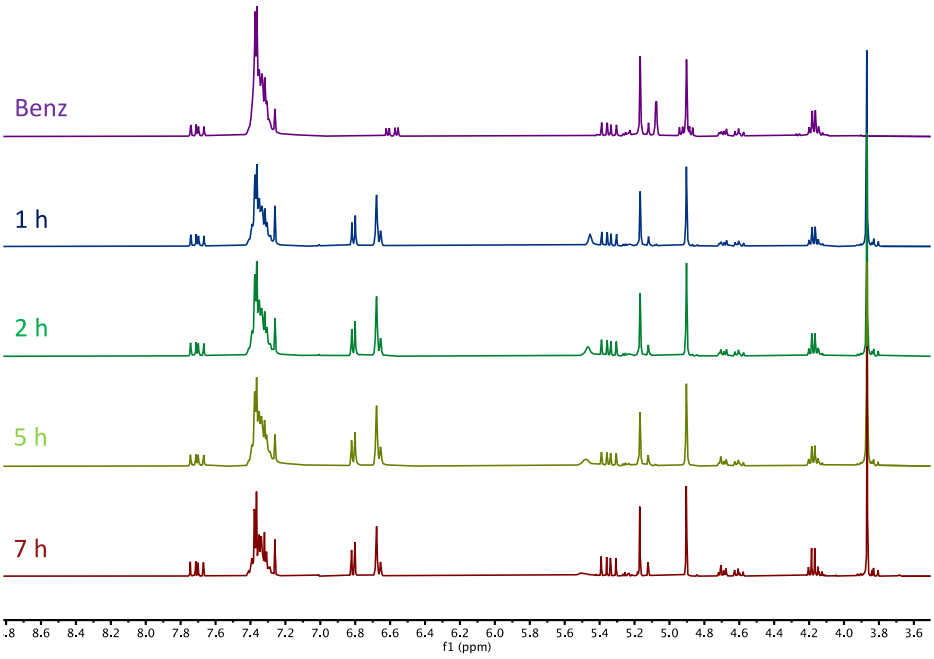

Figure S14. ^{1}H NMR sequence of Al-OH/G exchange reaction between Benz-VE and G in $CDCl_3$.

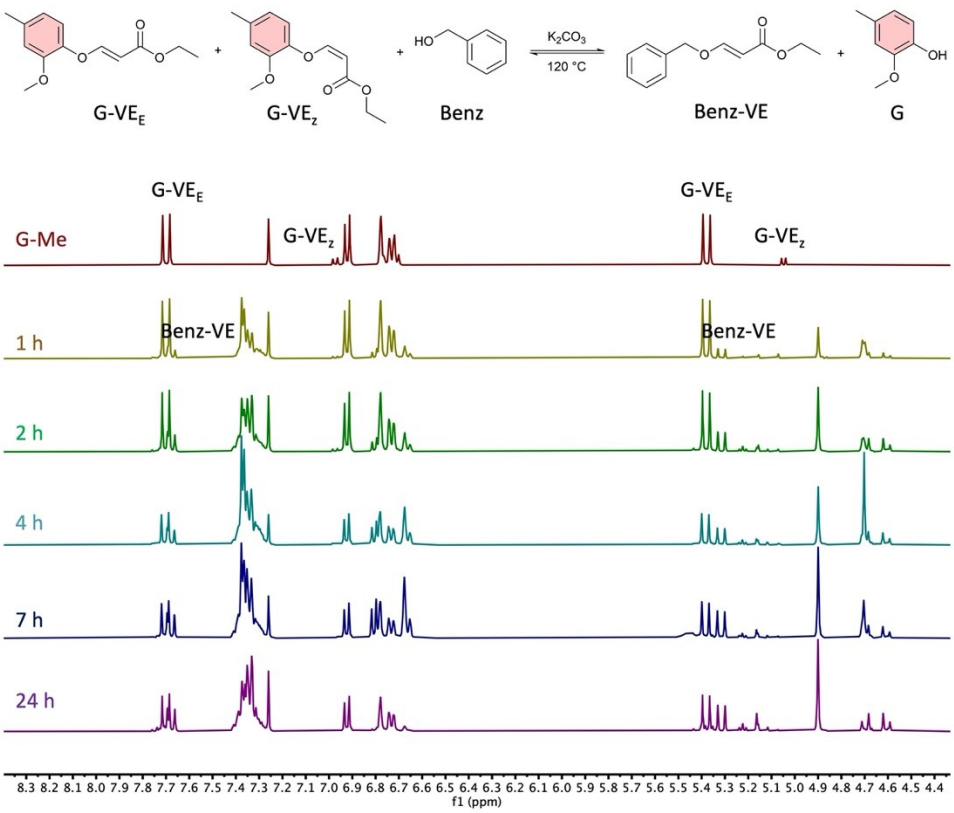

Figure S15. ^{1}H NMR sequence of G/Al-OH exchange reaction between G-VE and benzyl alcohol in $CDCl_3$.

Formation of alkyl and phenyl vinyl ether: study on small molecule models

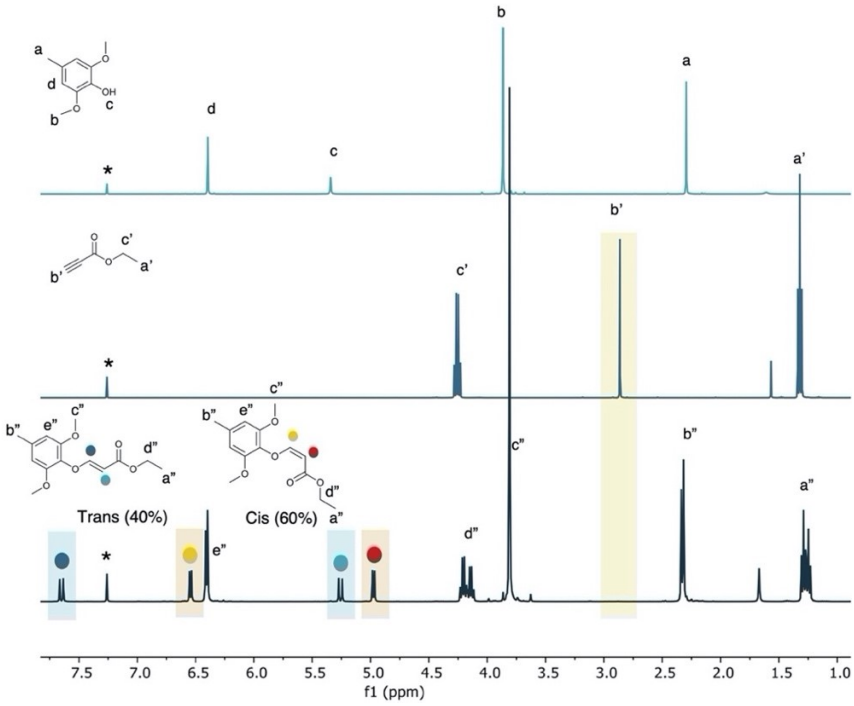

Figure S16. Stacked ^{1}H NMR spectra in $CDCl_3$ of S, ethyl propiolate and S-VE, from top to bottom.* = solvent.

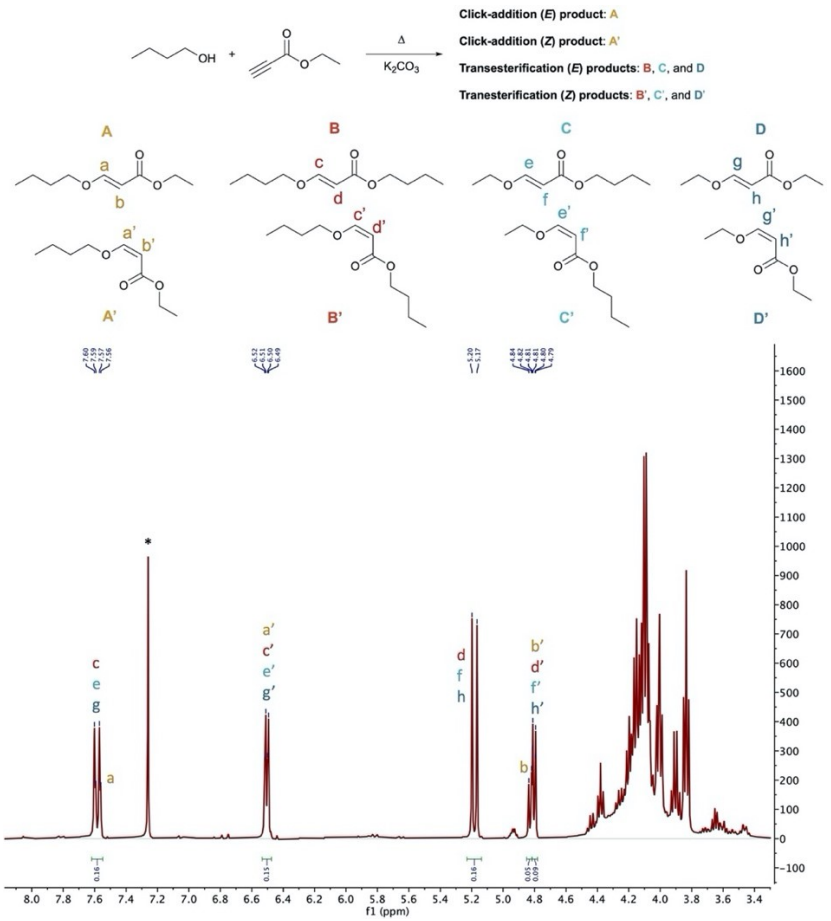

Figure S17. ^{1}H NMR of the reaction of 1-butanol with ethyl propiolate at 120 °C in $CDCl_3$ and proposition for the attribution of possible product from click-addition and transesterification reactions.

Formation of alkyl and phenyl vinyl ether: study on lignins

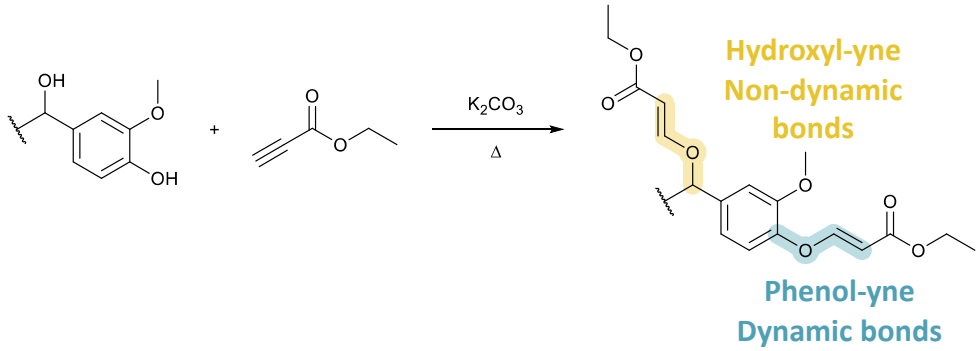

Scheme S3. Representation of dynamic and non-dynamic vinyl ether adducts on lignin.

Table S6. Reactional conditions of lignin modification with ethyl propiolate (EP) and conversion of Ph-OH and Al-OH.

Entry	Lignin	T (°C)	Solvent	Time (h)	m_{Lignin} (g)	V_{EP} (µL)	m_{K2CO3} (g)	Ph-OH converted (mmol g^{-1})	Al-OH converted (mmol g^{-1})	Conversion Ph-OH (%)	Conversion Al-OH (%)
OSL-80	OSL	80	DMF	23	1	293	0.02	1.26	0.43	43.7	24.8
KL-80	KL	80	DMF	23	0.5	219	0.015	2.93	1.10	67.8	44.0
KL-120	KL	120	DMF	4	0.5	219	0.015	3.01	1.11	69.6	44.2
OSL-DMSO	OSL	80	DMSO	23	1	293	0.02	1.40	0.40	48.6	23.2

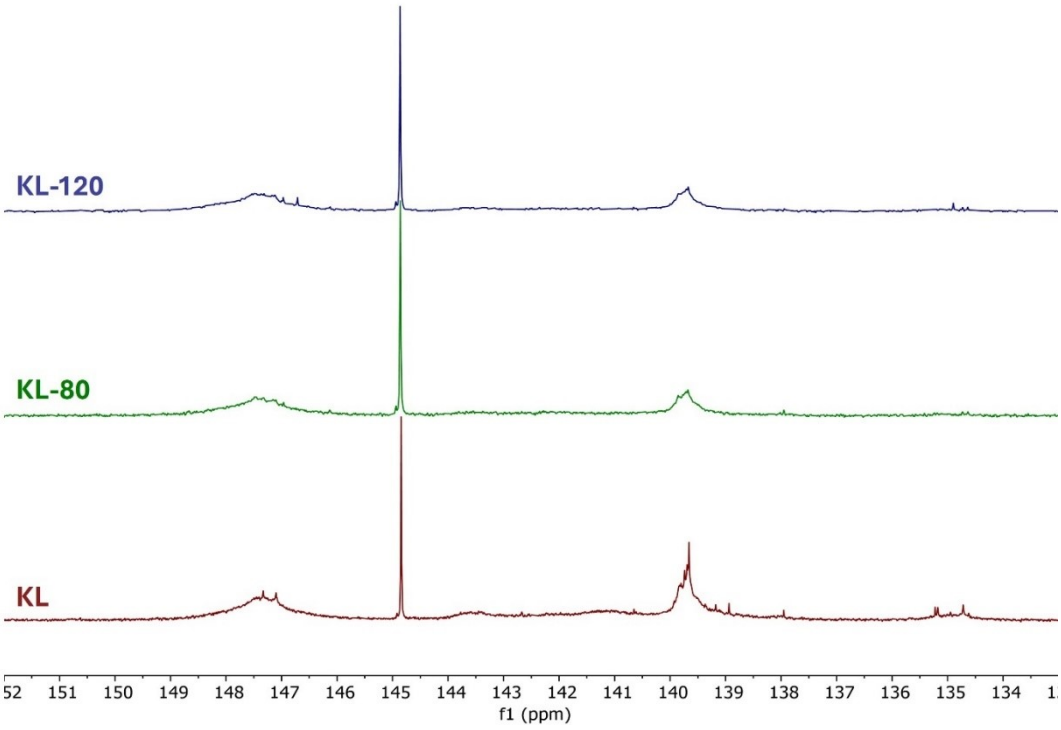

Figure S18. ^{31}P NMR spectra of KL and KL modified with EP in DMF at 80 or 120 °C (Table S6).

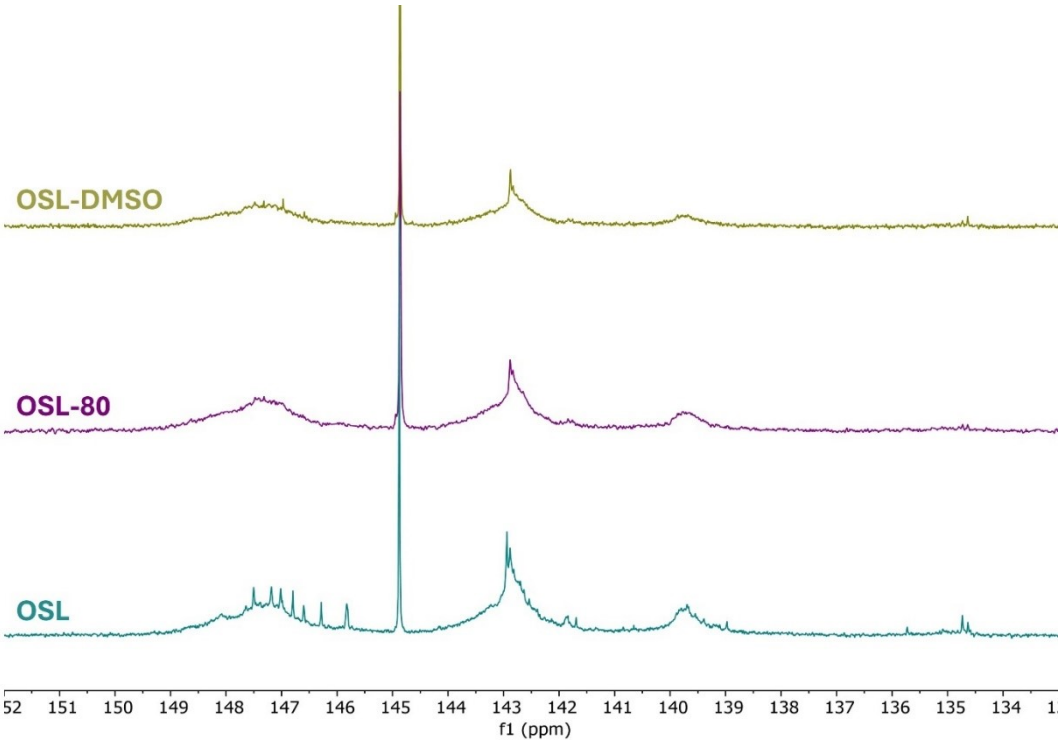

Figure S19. ^{31}P NMR spectra of OSL and OSL modified with EP at 80 °C in DMF or DMSO (Table S6).

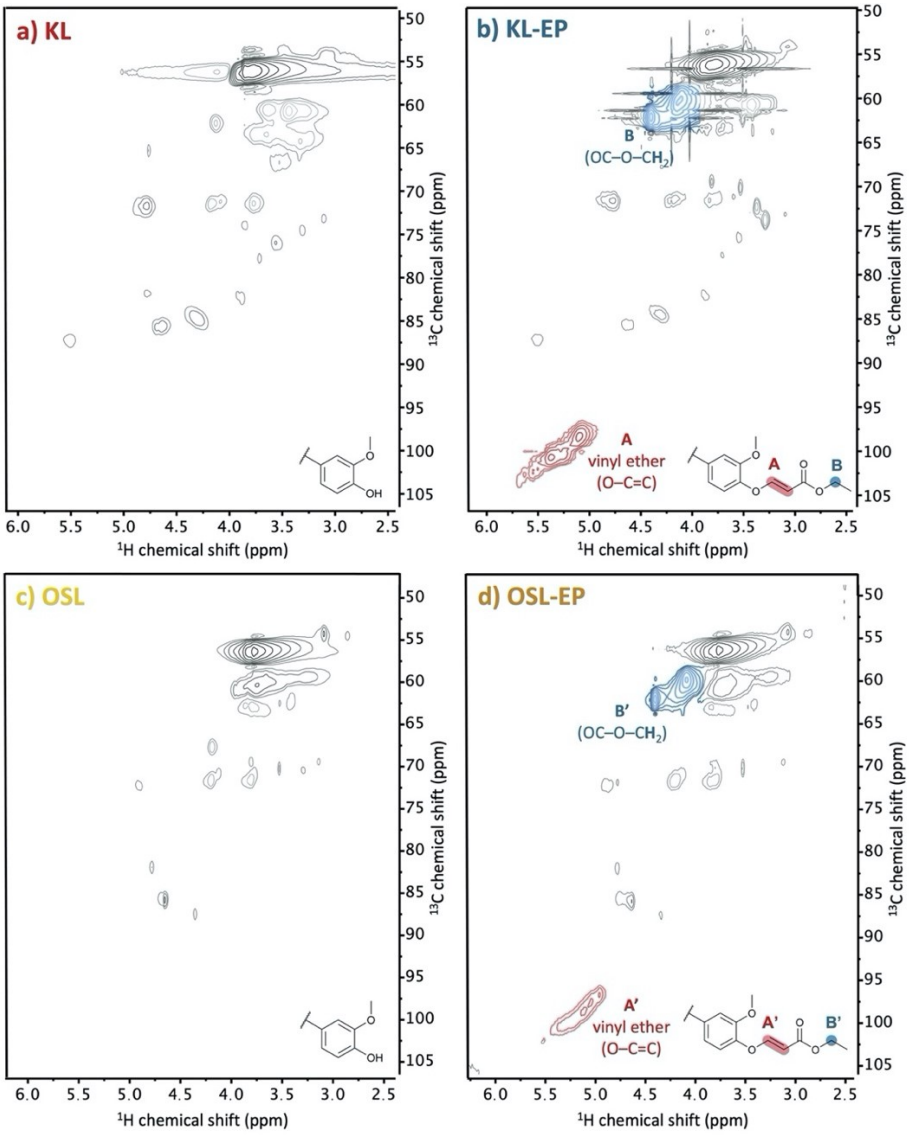

Figure S20. 2D HSQC spectra of a) KL, b) KL-EP, c) OSL, and d) OSL-EP in DMSO-d_6.

Synthesis of PEG-DA linker

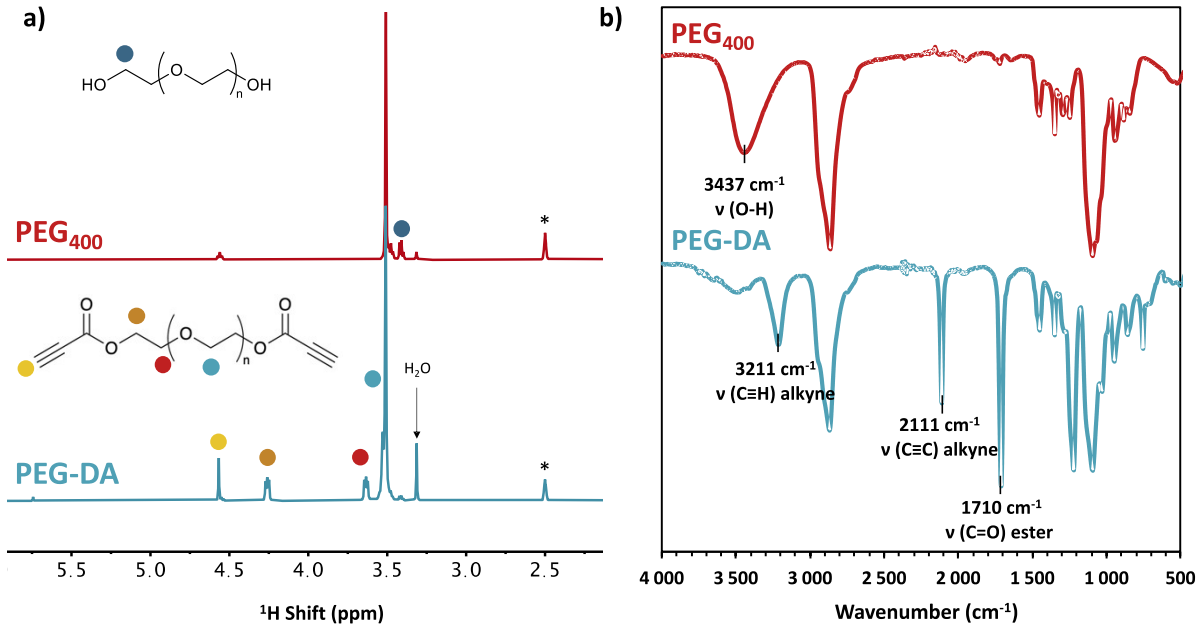

Figure S21. a) Stacked ^{1}H RMN in DMSO-d_6 and b) FT-IR spectra of PEG_{400} and PEG-DA.

The product of PEG_{400} Fischer esterification with propiolic acid was analyzed by ^{1}H NMR, as illustrated in Figure S21a. The conversion of PEG OH end groups was observed with the disappearance of the peaks at 3.41 ppm corresponding to the methylene next to OH end groups of PEG_{400}. New signals at 3.63 and 4.26 ppm were respectively attributed to methylene protons in α and β positions from the ester, confirming the grafting of ester moieties onto the PEG end chains [55]. Finally, the characteristic singlet of ethynyl protons appeared at 4.57 ppm confirming the grafting of alkyne moieties onto PEG_{400}. The amount of grafted alkyne measured by quantitative ^{1}H NMR using TCP as standard and was found to reach 2.22 mmol g^{-1} (Table S7).

The successful modification of PEG_{400} into PEG dialkyne (PEG-DA) was also confirmed by FT-IR, as displayed in Figure S21b. The effective grafting of alkyne moieties is showed by the emerging C≡C–H and C≡C bands at respectively 3211 and 2111 cm^{-1}, which are characteristic of alkyne functions [57]. A new C=O band associated with ester resulting from the esterification is observed at 1710 cm^{-1}. Finally, the strong decrease of the absorption vibration of OH groups at 3337 cm^{-1} is also indicative of the consumption of OH from PEG.

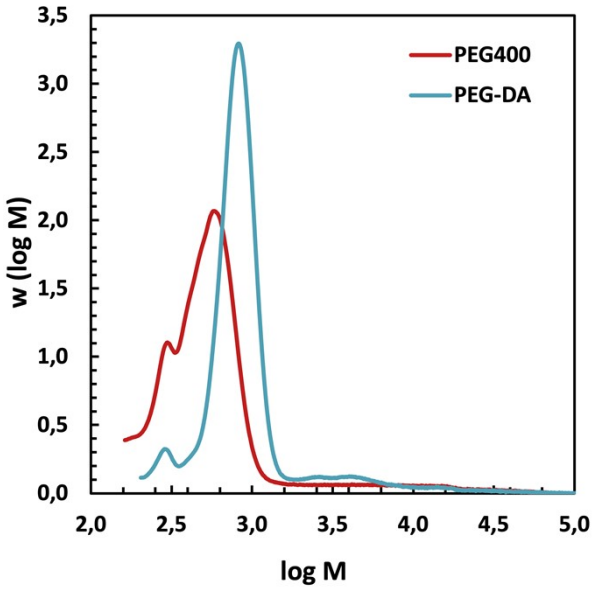

Figure S22. SEC curves of PEG_{400} and PEG-DA in THF.

PEG_{400} and PEG-DA were analyzed by SEC. The curves are displayed in Figure S22 and the physicochemical values (M_n, M_w and $Đ$) are reported in Table S7. M_n increased from 458 to 754 g mol^{-1} after esterification. M_w and $Đ$ slightly decreased from 2130 to 1950 g mol^{-1} and from 4.6 to 2.6, respectively. It is suspected that the variation of M_w and $Đ$ are resulting from interaction of PEG_{400} OHs with the column using ethylene bridge hybrid technology, whereas PEG-DA is less subjected to such interactions with the column.

Table S7. Physicochemical values of PEG_{400} and PEG-DA.

Designation	**OH content (mmol g^{-1})**	**DA content (mmol g^{-1})**	**M_n (g mol^{-1})**	**M_w (g mol^{-1})**	**Đ**
PEG_{400}	5.47	-	458	2130	4.6
PEG-DA	-	2.22	754	1950	2.6

Synthesis of lignin-based vitrimers

Table S8. Conditions of synthesis of lignin-based materials.

Material Designation	Lignin	Ph-OH content (mmol g^{-1})	m_{lignin} (g)	m_{PEG-DA} (g)	m_{K2CO3} (g)
KL-PY	Kraft	4.33	5.500	8.569	0.658
OSL-PY	Organosolv	2.89	8.000	8.318	0.639
DOSL-PY	Depolymerized organosolv	3.27	8.000	9.417	0.723

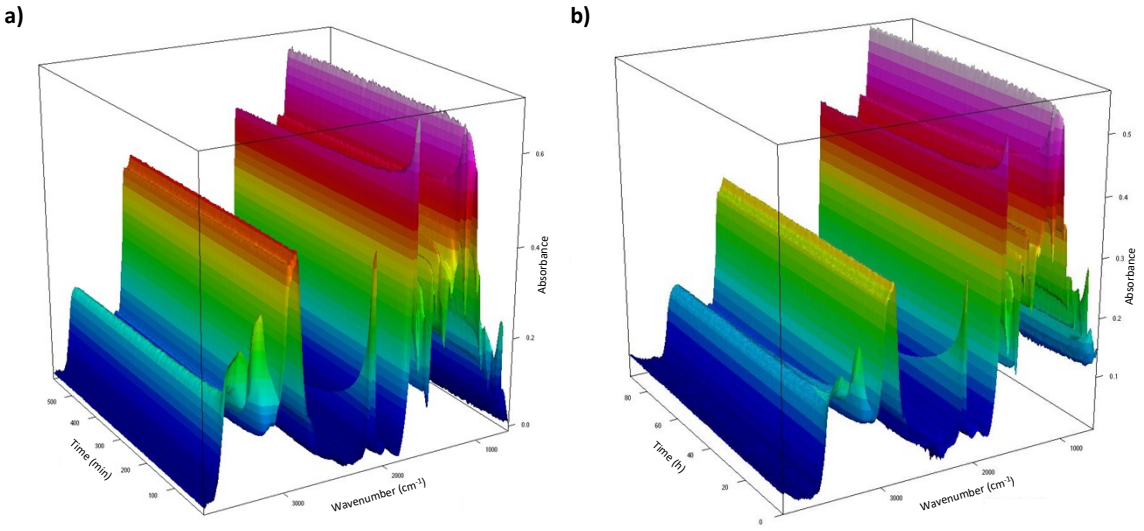

Figure S23. 3D view of the kinetic monitoring of the click addition by FT-IR at a) 120 °C and b) 80 °C.

Study of the influence of click addition reaction of KL with PEG-DA on the relaxation time

Two parameters were varied in the synthesis of KL-based networks, such as i) the amount of excess Ph-OH available to induce addition/elimination rearrangements, and ii) the molar equivalents of catalyst (K_2CO_3).

Since dynamic materials with recycling potential are designed, stress relaxation tests were performed at 190 °C to determine the impact of materials architecture on the dynamicity. The resulting curves were fitted with KWW model to determine their relaxation time τ*, as illustrated in Figure S24. The main relaxation parameters are available in Table S9, in SI. The free phenol content within the network was found to have a marginal influence on the stress relaxation. For instance, no difference is observed between 0.3 and 0.4 equivalents. Moreover, at 0.4 equivalents the material was extremely brittle due to higher lignin content. On the other hand, the amount of catalyst showed to strongly influence the network rearrangement. By increasing K_2CO_3 content from 0.05 to 0.2 equivalents, the relaxation time decreased significantly from 3783 to 1238 s. In these catalytic conditions, the material with 0.2 equivalents of free Ph-OH was found to relax faster than the one containing 0.3 equivalents of free Ph-OH. It is assumed to arise from its slightly lower lignin content, facilitating segmental mobility and favoring addition/elimination rearrangements. Finally, optimal rheological behavior was obtained for the network containing 0.2 equivalents of free Ph-OH and 0.2 equivalents of K_2CO_3 (τ* of 703 s). These conditions were then selected for the preparation of the final materials.

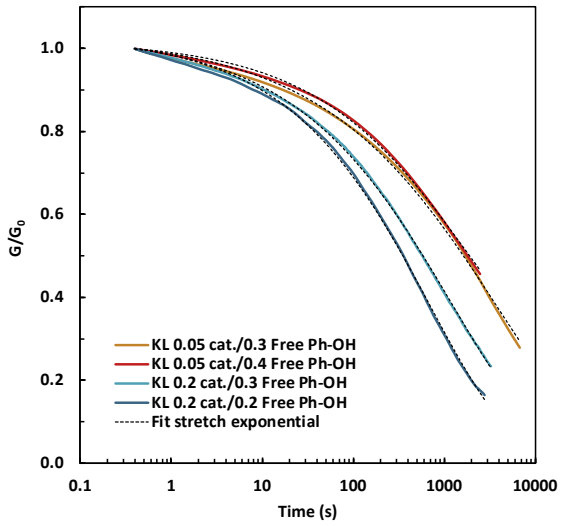

Figure S24. Stress relaxation curves obtained at 190 °C on materials synthesized with different experimental conditions: varying the amount of free Ph-OH (from 0.2 to 0.4 equivalents), and the catalyst equivalents (from 0.05 to 0.2).

Table S9. Relaxation parameters obtained at 190 °C varying the amount of free Ph-OH and the catalyst equivalents.

Entry	Free phenol equivalents	Catalyst equivalents	$\tau^*_{190\,°C}$ (s)	β
1	0.05	0.3	3783	0.39
2	0.05	0.4	1688	0.45
3	0.2	0.3	1239	0.43
4	0.2	0.2	703	0.47

Characterization of lignin-based vitrimers

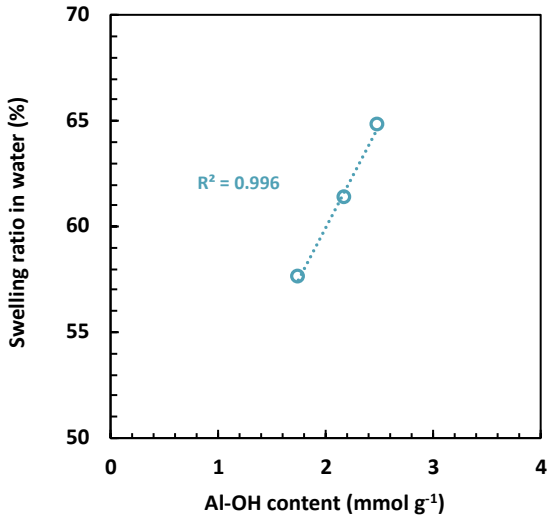

Figure S25. Evolution of swelling ratios in water with Al-OH content.

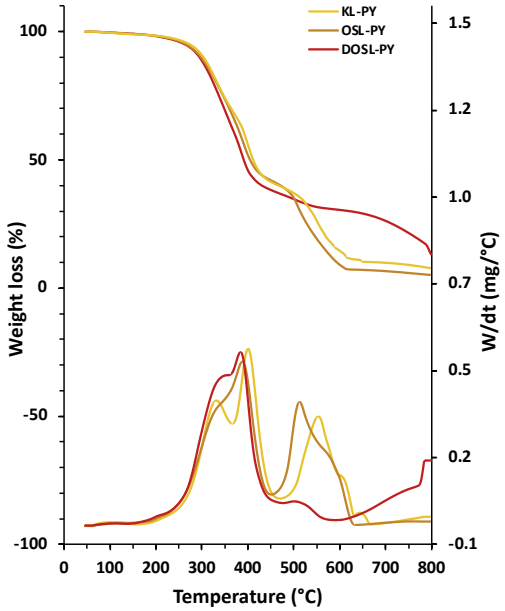

Figure S26. TGA curves of the materials.

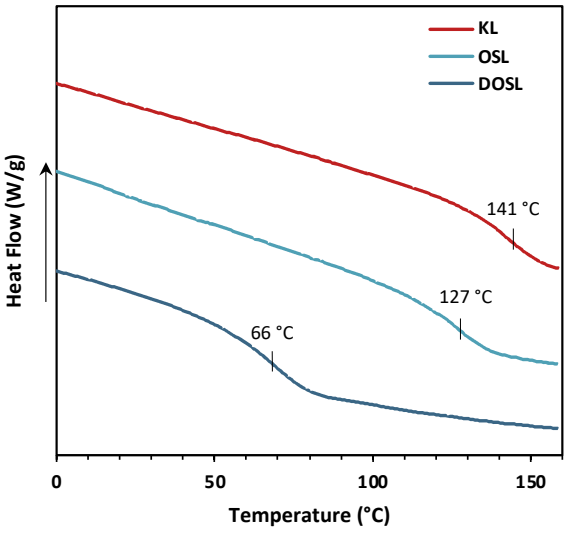

Figure S27. DSC curves of the different lignins.

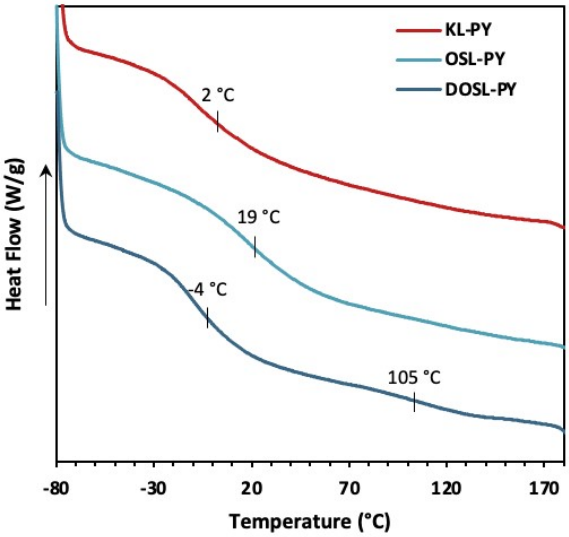

Figure S28. DSC curves of the series of materials.

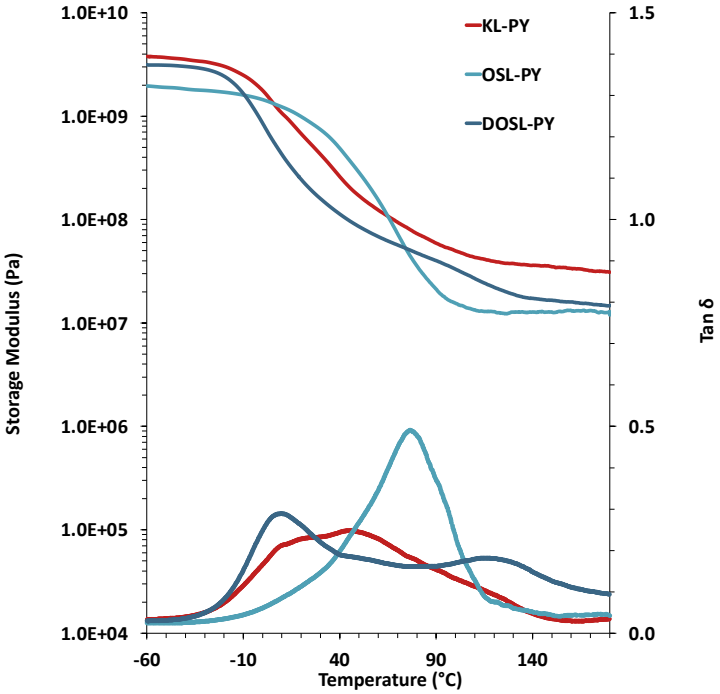

Figure S29. DMA curves of the materials.

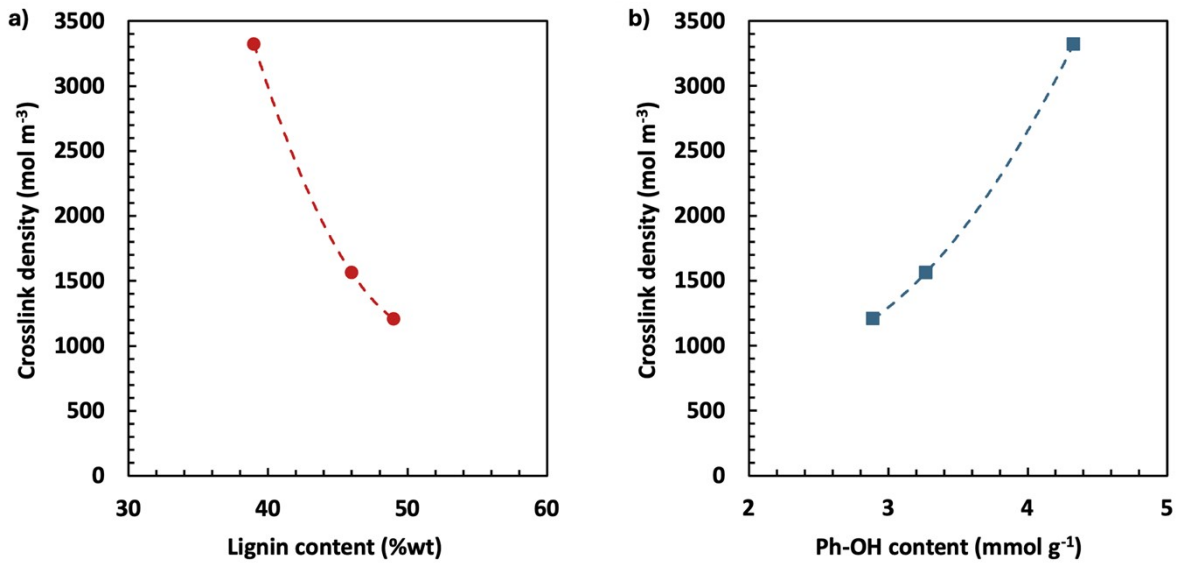

Figure S30. Evolution of the crosslink density as a function of a) the lignin content and b) the Ph-OH content of the lignins.

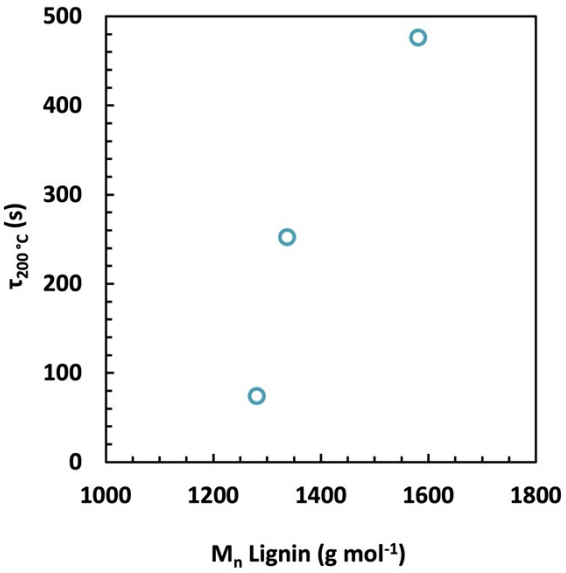

Figure S31. Evolution of the relaxation time at 200 °C with lignin molar mass.

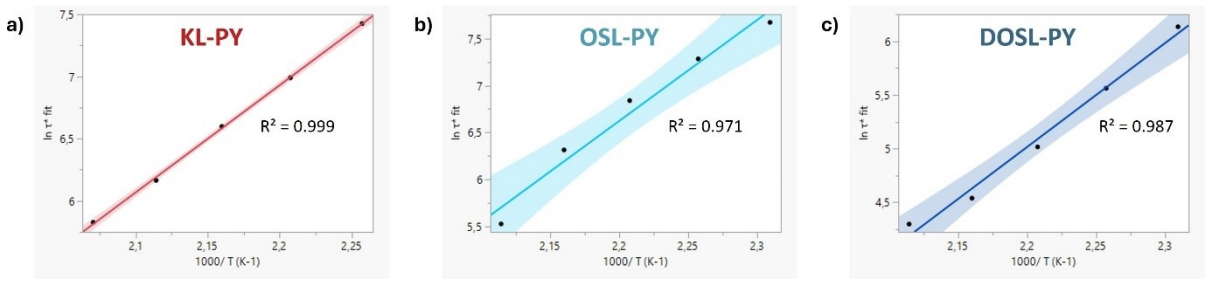

Figure S 32. Determination of activation energies (E_a) from the slopes of the Arrhenius plots for a) KL-PY, b) OSL-PY and c) DOSL-PY. The shaded areas represent the confidence intervals of the linear adjustments (α = 0.05), used to estimate the standard deviation of E_a.

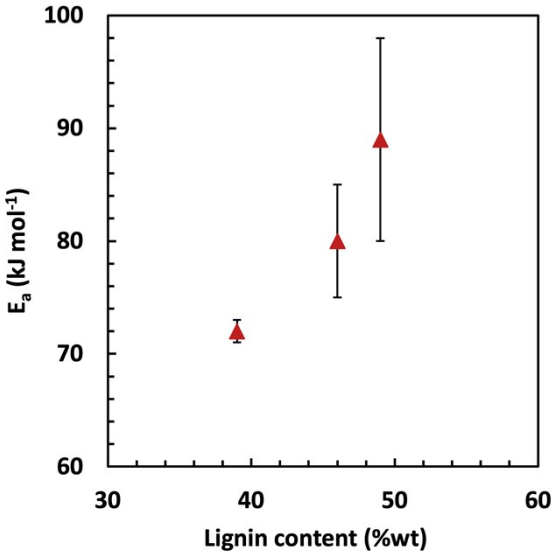

Figure S33. Evolution of E_a of the vitrimers with the lignin content.

Table S10. Parameters used for the calculation of T_v of each vitrimers. A and B represent the slope and y-intercept of the Arrhenius linear plots.

PY (Designations)	G'$_{rubbery}$ (Pa)	A	B	T_v (°C)
KL-PY	3.50E+07	8.608	-12.006	114
OSL-PY	1.27E+07	10.706	-16.928	107
DOSL-PY	1.65E+07	9.644	-16.199	81

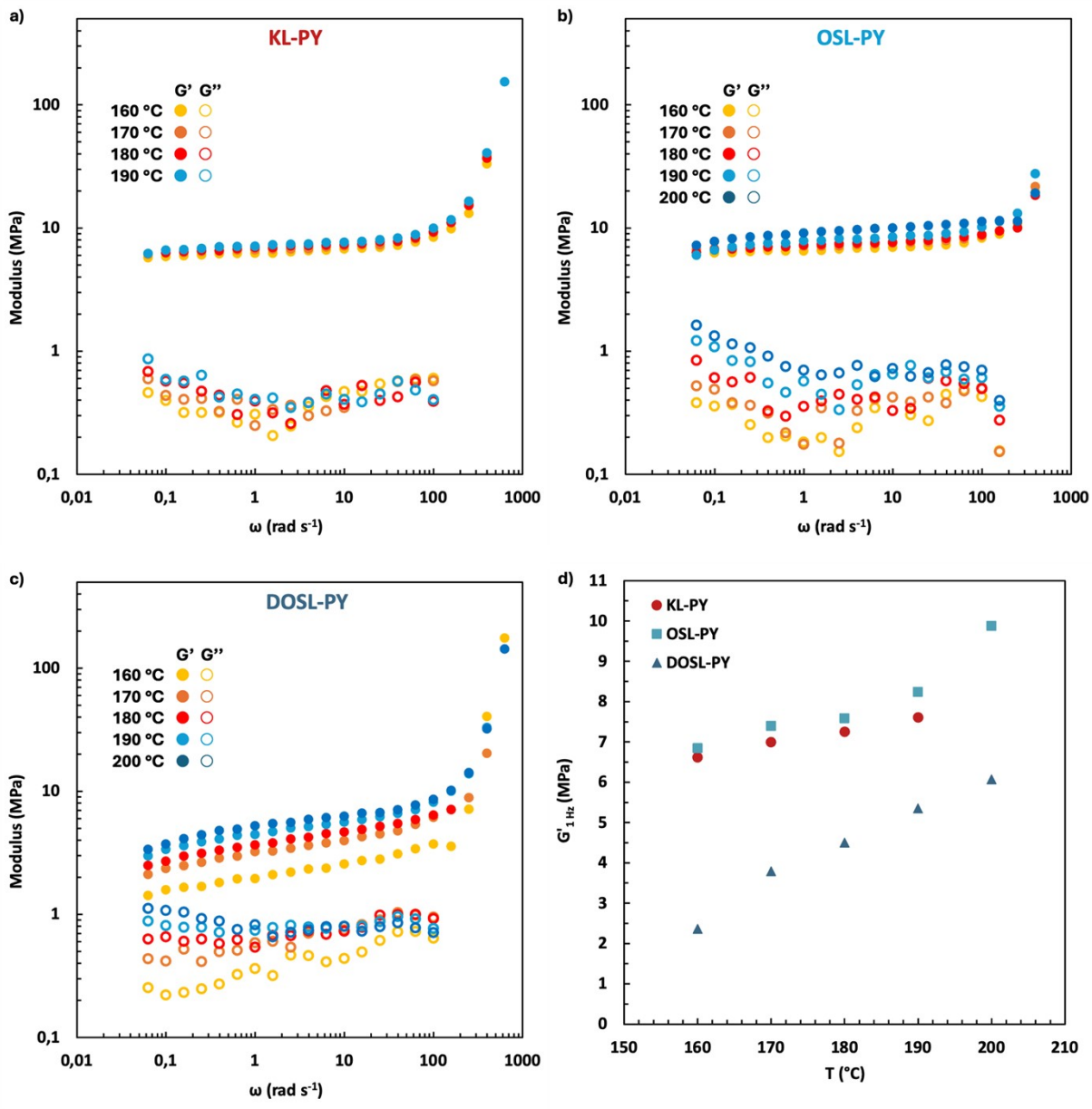

Figure S 34. Frequency sweep measurements at different temperatures of a) KL-PY, b) OSL-PY and c) DOSL-PY. d) Evolution of the modulus at 1 Hz with the temperature.

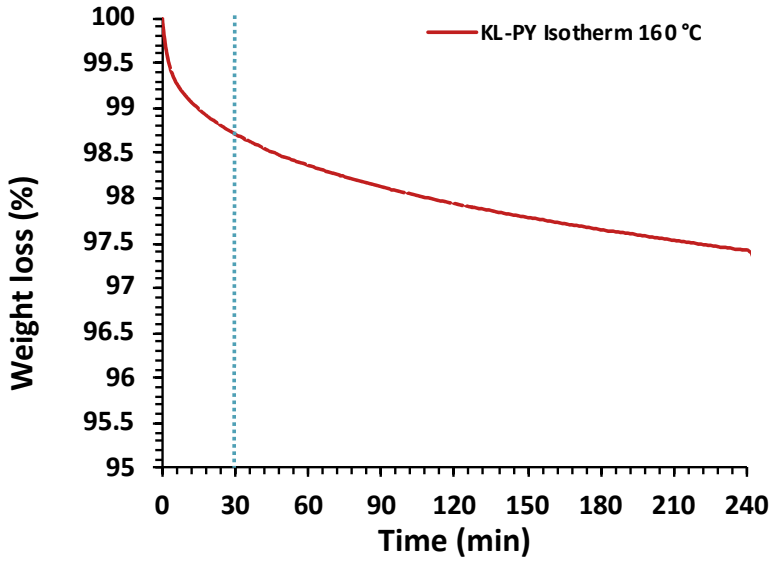

Figure S35. Curve of KL-PY thermal degradation under an isotherm at 160 °C for 4 h.

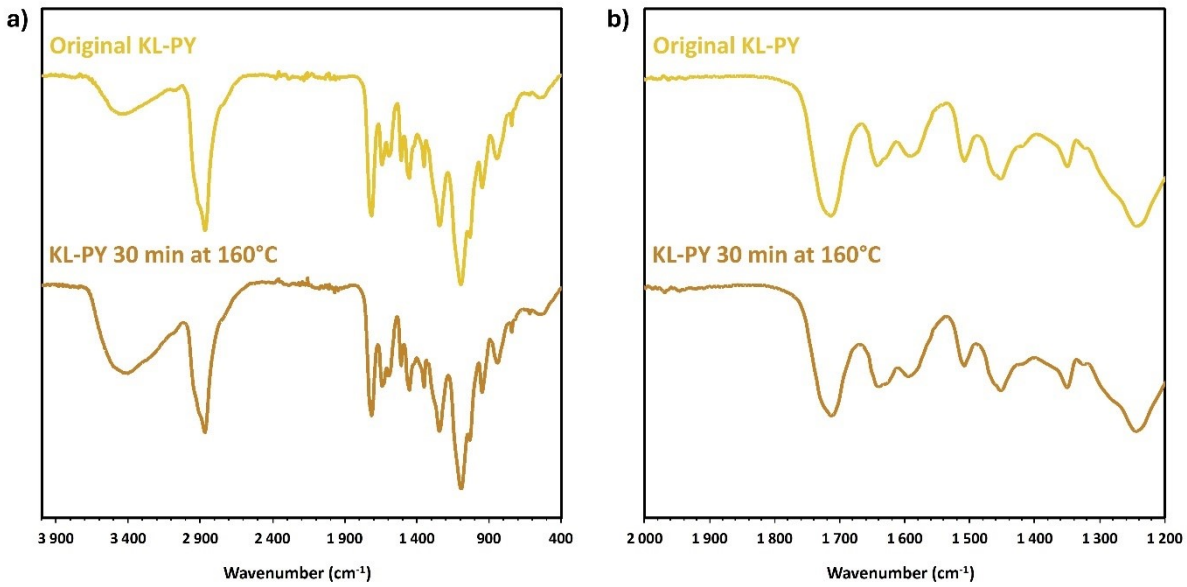

Figure S36. a) FT-IR spectra of pristine KL-PY and KL-PY after thermal treatment at 160 °C for 30 minutes. b) Detail of the 1200 – 2000 cm^{-1} region.

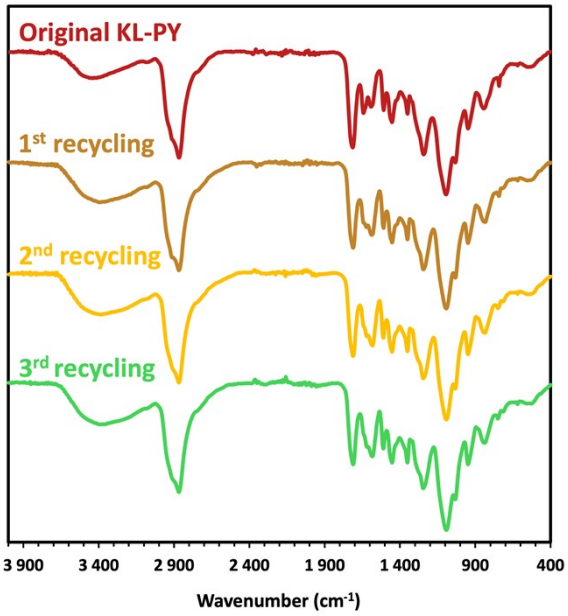

Figure S 37. FT-IR spectra of pristine and recycled KL-PY.

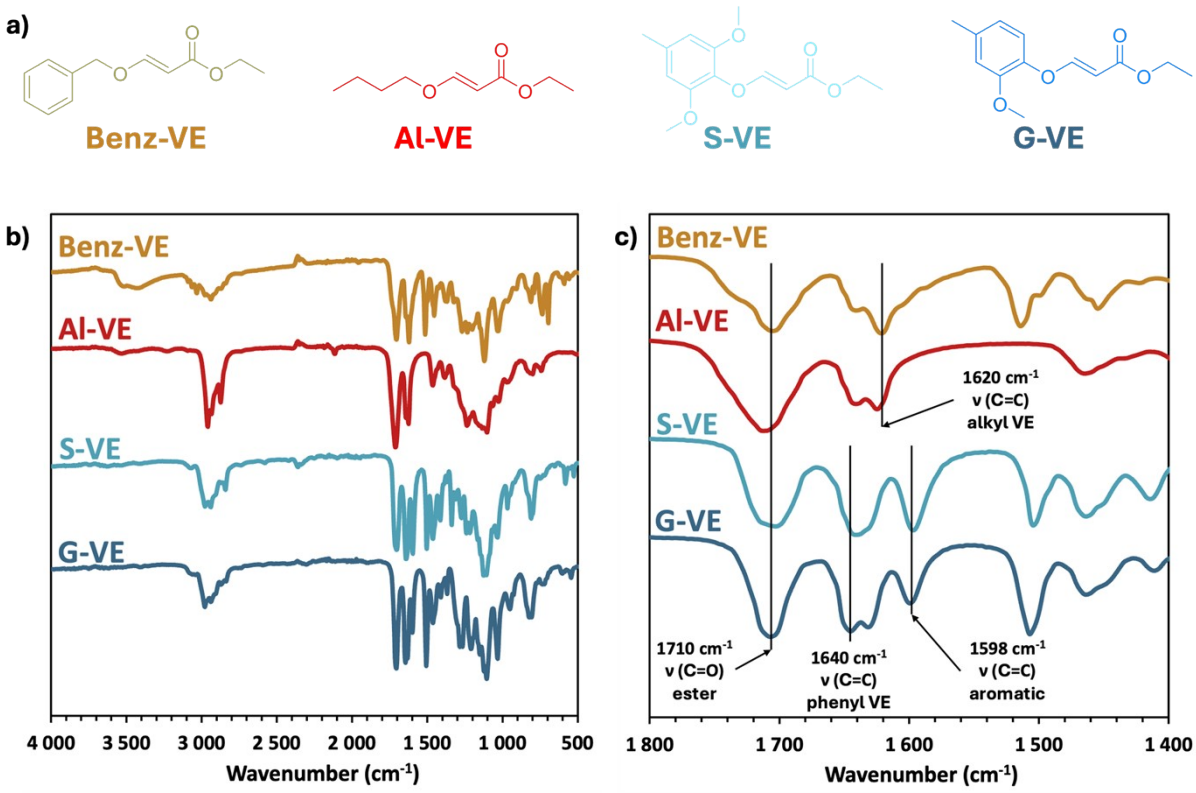

Figure S38. a) Structures of aliphatic and aromatic vinyl ether models. b) Full FT-IR spectra of corresponding models and c) detail of the 1400 – 1800 cm^{-1} region.

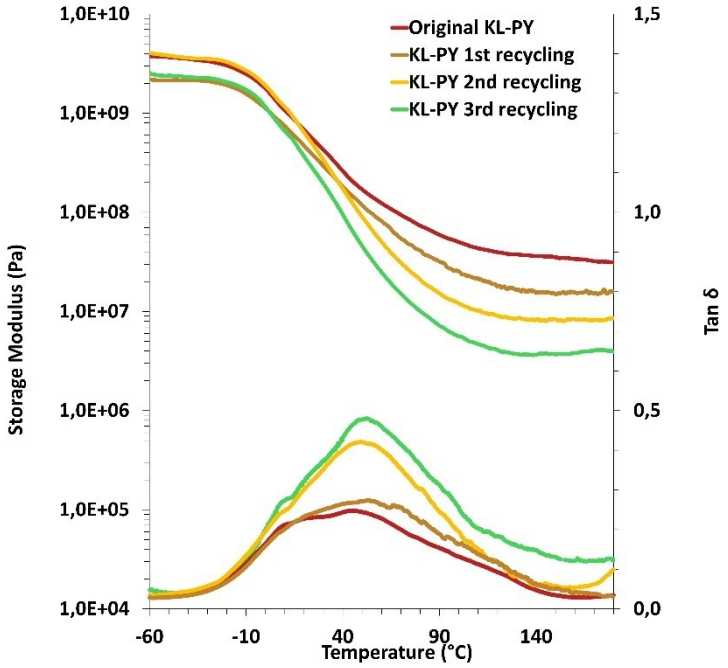

Figure S39. DMA curves of pristine and recycled KL-PY.

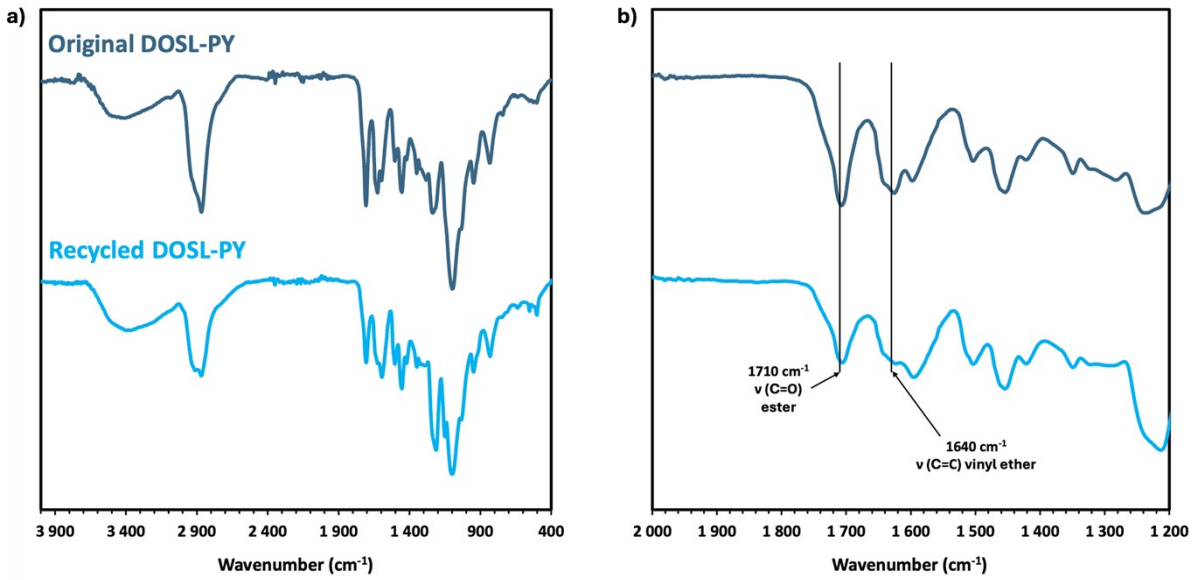

Figure S40. a) FT-IR spectra of pristine and recycled DOSL-PY. b) Detail of the 1200 – 2000 cm^{-1} region.

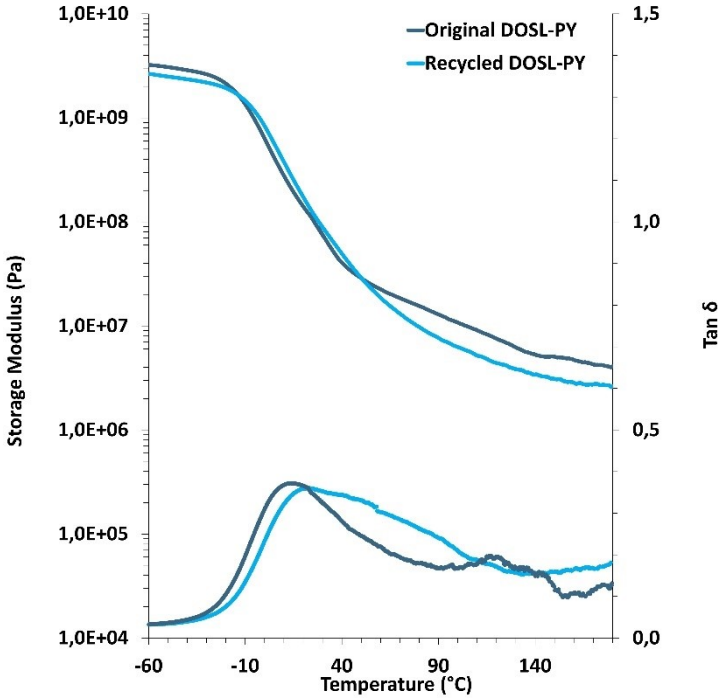

Figure S41. DMA curves of pristine and recycled DOSL-PY.

Table S11. Depolymerization tested conditions on OSL.

Entry	Sample concentration (mg mL^{-1})	Solvent	T (°C)	Observed solubilization?
1	10	HCl 2M	60	No
2	7.75	Acetone/HCl 2M (7:3)	60	No
3	7.75	Acetone/HCl 2M (7/3) + 2 drops HCl 37%	60	Yes
4	12	DMSO/HCl 1M (8:2)	70	Yes

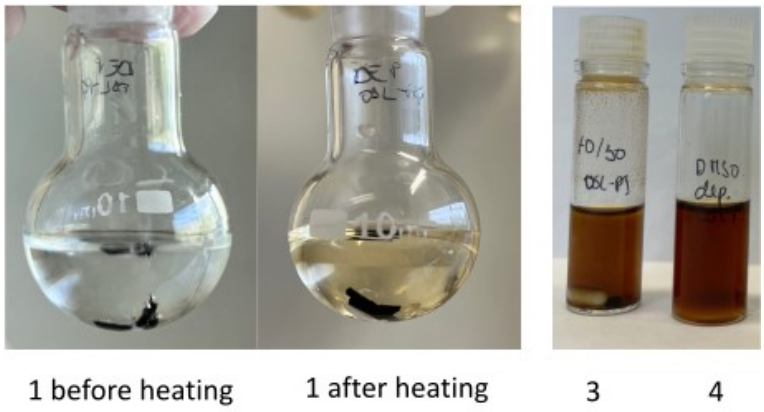

Figure S42. Pictures of the tested depolymerization conditions.

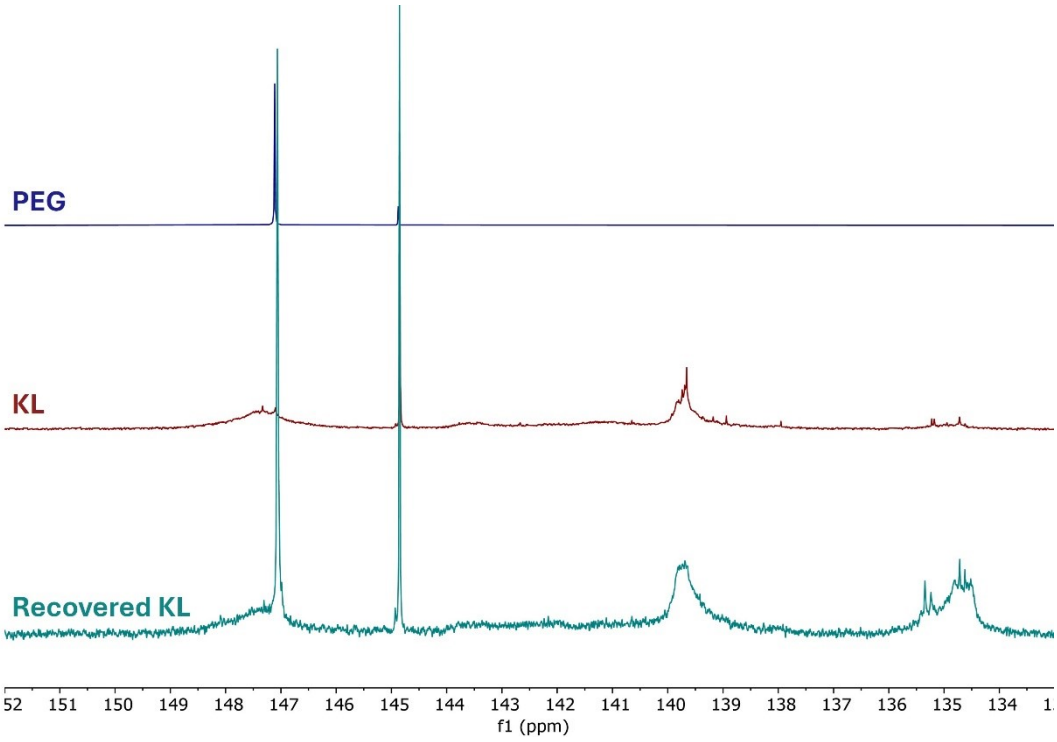

Figure S43. Stacked ^{31}P NMR of pristine and chemically recovered KL. Spectrum of PEG is given for comparison.

Table S12. Physicochemical properties of pristine and recovered KL.

Lignin (Designations)	**Ph-OH content**	M_n (g mol^{-1})	M_w (g mol^{-1})	$Đ$

	(mmol g^{-1})			
Pristine KL	4.33	1580	5270	3.3
Recovered KL	1.62	1520	4040	2.7

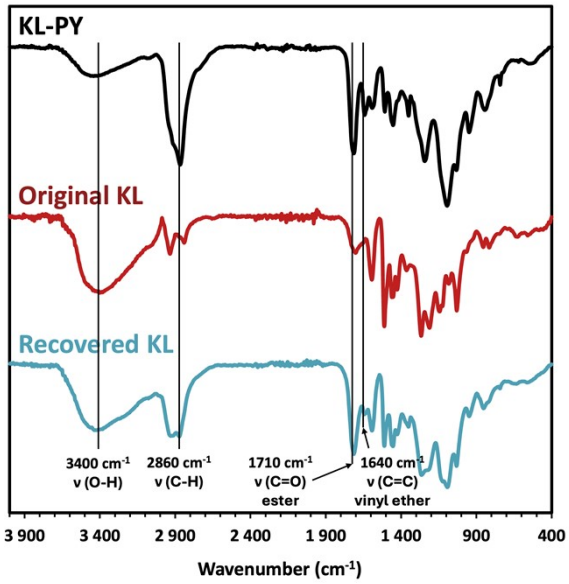

Figure S44. Stacked FT-IR spectra of KL-PY, pristine KL, and recovered KL.

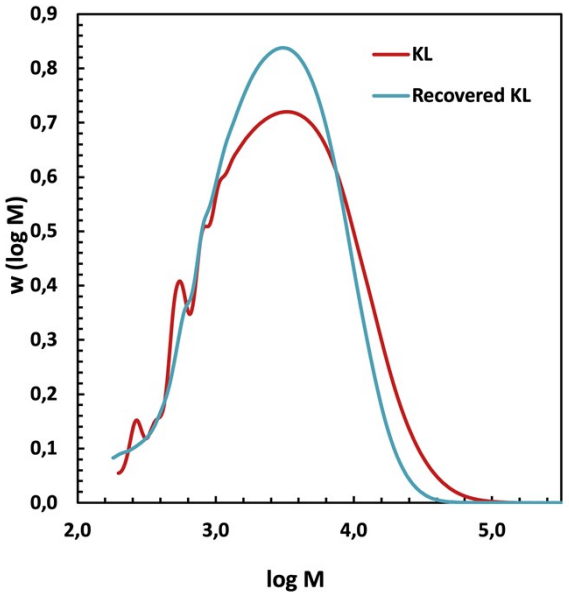

Figure S45. SEC curves of pristine and recovered KL.